Novel Data Detection and Channel Estimation Algorithms for BICM-OFDMA Uplink Asynchronous Systems in the Presence of IQ Imbalance

Mohamed Marey, *Senior Member, IEEE*, and Heidi Steendam, *Senior Member, IEEE*

***Abstract*—The problem of channel estimation and in-phase/quadrature-phase (IQ) imbalance is one of the main challenges that has to be faced by uplink transmission in orthogonal frequency division multiple access (OFDMA) systems. The previously reported investigations for such systems are limited to synchronous and uncoded transmission. Furthermore, in these previous works, equalization of the IQ imbalance should be performed after the estimation process in order to properly detect data symbols. In this contribution, the transmit and receive IQ imbalance for uplink OFDMA systems is investigated in the context of asynchronous and bit-interleaved coded modulation (BICM) transmission. We propose a novel data detector exploiting the unwanted IQ as a beneficial resource to achieve a diversity gain, without the necessity of an additional equalizer. In addition, we develop a novel code-aided algorithm to estimate the propagation delays and the overall channel impulse responses (CIRs), which include the physical CIRs and IQ imbalance occurring at both the transmitters and base station. Since the exact maximum-likelihood (ML) solution to this problem turns out to be too complex for practical purposes, we resort to the space alternating generalized expectation-maximization (SAGE) algorithm as a low complexity method to perform parameter estimation. The proposed estimation algorithm operates in an iterative way, in which the soft information provided by the channel decoder is utilized as a priori information to refine the estimates. The computational complexity analysis and simulation results confirm the effectiveness of the proposed estimation algorithm and the proposed detector for practical application.**

***Index Terms*—OFDMA, IQ imbalance, SAGE algorithm, BICM.**

I. Introduction

ORTHOGONAL frequency division multiple access (OFDMA) has recently received a significant amount of attention as a promising technique to fulfill the high data rate demand for future wireless communication systems. OFDMA has significant advantages in terms of high spectrum efficiency, robustness against frequency-selective fading channels, resistance to multi-access interference (MAI), and simplified equalization. Furthermore, it allows straightforward dynamic sub-carrier assignment to support variable quality of service requirements of the individual users. OFDMA has become the physical layer of choice for many wireless communication systems such as worldwide interoperability for microwave access (WiMAX), long-term evolution (LTE), and IEEE 802.11 [1], [2]. An appealing feature of OFDMA is that the transmitted signals of different users are orthogonal and that MAI can be avoided. This makes OFDMA attractive for uplink transmission as the receiver at the base station can easily separate each user's signal in the frequency domain. However, propagation delay and channel estimation is a real challenging issue in OFDMA uplink transmission because each user has its own delay and channel impulse response (CIR). It is not surprising that a massive amount of research has been devoted to this problem (e.g., [3]–[6]).

The direct conversion architecture has been widely used in telecommunication because of its low complexity and cost [7], [8]. Nevertheless, it introduces impairments such as in-phase/quadrature-phase (IQ) imbalance, incurring a severe degradation in communication performance. The IQ imbalance is basically the mismatch between the I and Q branches from the ideal case, i.e., from the exact 90 degree phase difference and equal amplitude between the sine and cosine branches. Estimation and compensation of IQ imbalance has become a topic of extensive research in the wireless domain. Due to the narrow spacing and spectral overlap between the sub-carriers, orthogonal frequency division multiplexing (OFDM) systems are much more sensitive to the IQ imbalance than single-carrier systems. This leads to a loss of sub-carrier orthogonality, which translates into inter-carrier interference (ICI) and results in a degradation of the performance. The influence, estimation, and compensation of IQ imbalance for single-user OFDM systems have been treated in a massive amount of publications, see e.g., [9]–[19] and the references therein.

To the best of the authors' knowledge, there are only two works in the literature that devoted to the problem of the IQ imbalance for uplink OFDMA systems [20], [21]. The authors in [20] propose zero forcing and minimum mean square error equalizers for uplink OFDMA and single-carrier frequency-division multiple access systems affected by transmit IQ imbalance; however, they assumed perfect knowledge about the channel and transmit IQ imbalance. The authors in [21] develop a data-aided algorithm to estimate the channel and transmit IQ using a two-dimensional least square estimation criterion; they also employ a zero-forcing equalizer to recover the data symbols. The previous works [20], [21] assume that there is no receive IQ imbalance; however, a realistic

Manuscript received April 25, 2013; revised September 6, 2013; accepted January 15, 2014. The associate editor coordinating the review of this paper and approving it for publication was S. Wei.

M. Marey is with the Faculty of Electronic Engineering, Menoufyia University, Menouf, 32952, Egypt (e-mail: mfmmarey@mun.ca).

H. Steendam is with the Department of Telecommunications and Information Processing, Ghent University, Belgium (e-mail: hs@telin.ugent.be).

Digital Object Identifier 10.1109/TWC.2014.033114.130726

1536-1276/14$31.00 © 2014 IEEE

system model of an OFDMA system must consider both the transmit and receive IQ imbalance. In addition, they assume uncoded and synchronous transmission; however, practical systems typically employ error correcting codes and consider asynchronous transmission as the users' signals reach the base station with different propagation delays. Furthermore, data detection in the previous works [20], [21] requires an equalizer to cancel out the effects of the IQ transmit imbalance; this comes at the cost of computational complexity at the receiver[1].

In this work, we relax the previous assumptions and introduce another approach to handle the transmit and receive IQ imbalance for uplink OFDMA systems associated with asynchronous and bit-interleaved coded modulation (BICM) transmission. The novelty of this work lies in the following two points.

- Instead of using a family of algorithms to separately estimate (or calibrate) the transmit and receive IQ imbalance along with the channel and propagation delay for each user, we propose a novel code-aided algorithm to jointly estimate these parameters. We combine the IQ effects at each transmitter and the receiver with the physical CIR into one parameter referred to as the overall CIR. The maximum-likelihood (ML) principle is employed to estimate the propagation delays and the overall CIRs via the space-alternating generalized expectation-maximization (SAGE) algorithm [22]. In our approach, we do not need additional equalization to compensate for the transmit and receive IQ imbalance, as it is included in the overall CIRs.
- We use the IQ imbalance of the transmitters as a valuable resource to obtain an additional diversity gain (on top of the diversity gain obtained from other sources), and design the optimal demapper for asynchronous uplink BICM-OFDMA systems.

The remainder of the paper is organized as follows. Section II presents the signal model and problem formulation. The estimation algorithm is proposed in Section III. In Section IV, the proposed BICM decoder is introduced. In Section V, the computational complexity analysis of the proposed estimator and detector is derived. Simulation results are provided in Section VI. Finally, Section VII draws the conclusions.

II. Signal Model and Problem Formulation

We consider an uplink OFDMA system with K active users and a destination node which serves as a base station, as indicated in Figure 1. The total number of sub-carriers, N, is divided into Q sets; each of them has V sub-carriers ($V = N/Q$) and is exclusively used by one user ($K \leq Q$). Frame-based transmission is assumed, in which frames consisting of M OFDMA blocks are transmitted for each user. A frame intended for the kth user is generated as follows. A block of $\mathbf{b}^{(k)} = \left[b_0^{(k)}, \cdots, b_{N_b-1}^{(k)}\right]$ information bits is encoded, resulting in N_c coded bits. After interleaving, these coded bits are mapped to a sequence of N_d symbols, belonging to a unit-energy χ-point constellation Ω (with $N_d = N_c/\chi$). After insertion of N_p pilot symbols, we obtain a sequence $\mathbf{d}^{(k)} = \left[d^{(k)}(0), \cdots, d^{(k)}\left(N_d + N_p - 1\right)\right]$. Now, $\mathbf{d}^{(k)}$ is broken down into M blocks of length P where $P = \left(N_d + N_p\right)/M$ and $P \leq V$. The M data blocks are buffered and converted, one at a time, to OFDMA blocks. The mth data block of the kth user, $\mathbf{d}_m^{(k)} = \left[d_m^{(k)}(0), \cdots, d_m^{(k)}\left(P-1\right)\right]$, is converted into an OFDMA block as follows. Each data symbol, $d_m^{(k)}(p)$, is assigned to a unique sub-carrier, $u^{(k)}(p)$, belonging to the sub-carrier set, $\mathbf{U}^{(k)}$, of user k. Sub-carriers outside the set $\mathbf{U}^{(k)}$ are padded with zeros. As we will show in Section IV, in order to exploit the IQ imbalance as a beneficial resource to achieve a diversity gain, we assume that the sub-carrier $u^{(k)}(p)$ and its mirror $-u^{(k)}(p)$ are used as active sub-carriers. This can easily be incorporated in many existing OFDMA frequency assignment schemes, such as the interleaved sub-carrier assignment. After that, an N-point inverse discrete fast Fourier transform (IFFT) is performed and a ν-point cyclic prefix (CP) is included to produce the corresponding samples of the time-domain OFDMA block, $\mathbf{x}_m^{(k)} = \left[x_m^{(k)}(-\nu), \cdots, x_m^{(k)}(N-1)\right]$. Mathematically, $x_m^{(k)}(n)$ can be expressed as

$$x_m^{(k)}(n) = \frac{1}{\sqrt{N}} \sum_{p=0}^{P-1} d_m^{(k)}(p) e^{j2\pi n u^{(k)}(p)/N}, -\nu \leq n \leq N-1. \tag{1}$$

Accordingly, we can write the undistorted transmitted frame from user k as

$$\vec{\mathbf{x}}^{(k)} = \left[\mathbf{x}_0^{(k)}, \mathbf{x}_1^{(k)}, \mathbf{x}_2^{(k)}, \cdots, \mathbf{x}_{M-1}^{(k)}\right]. \tag{2}$$

Following [7], the distorted frame transmitted by user k, $\underline{\mathbf{x}}^{(k)}$, can be given as

$$\underline{\mathbf{x}}^{(k)} = \boldsymbol{\alpha}_{Tx}^{(k)} \vec{\mathbf{x}}^{(k)} + \boldsymbol{\beta}_{Tx}^{(k)} \vec{\mathbf{x}}^{(k)*}, \tag{3}$$

where $\boldsymbol{\alpha}_{Tx}^{(k)}$ and $\boldsymbol{\beta}_{Tx}^{(k)}$ are the distortion parameters related to the amplitude and phase imbalance between the I and Q branches for the transmit antenna of user k, respectively. In the frequency-flat IQ imbalance model, $\boldsymbol{\alpha}_{Tx}^{(k)}$ and $\boldsymbol{\beta}_{Tx}^{(k)}$ can be written as[2] [7]

$$\boldsymbol{\alpha}_{Tx}^{(k)} = \cos\phi_{Tx}^{(k)} + j\varepsilon_{Tx}^{(k)} \sin\phi_{Tx}^{(k)}, \tag{4a}$$

$$\boldsymbol{\beta}_{Tx}^{(k)} = \varepsilon_{Tx}^{(k)} \cos\phi_{Tx}^{(k)} + j \sin\phi_{Tx}^{(k)}, \tag{4b}$$

where $\epsilon_{Tx}^{(k)}$ and $\phi_{Tx}^{(k)}$ are the IQ gain and phase offset at the transmit antenna of user k, respectively, and $j = \sqrt{-1}$. The frame $\underline{\mathbf{x}}^{(k)}$ propagates to the base station through a wireless channel $\mathbf{h}^{(k)} = \left[h^{(k)}(0), \cdots, h^{(k)}(L-1)\right]$, with L denoting the maximum number of sample-spaced channel taps among all the transmit receive antenna pairs. We assume a quasi-static block-fading channel that remains constant during each frame but can vary independently from frame to frame. As the locations of the users are different, their signals reach the base station with different propagation delays. Without loss of generality, the propagation delay of user k can be split into an integer part $\tau^{(k)}$ and a fractional part $\epsilon^{(k)}$ with respect to the sampling period. The fractional part can be

[1]We notice that in [20], [21] a diversity gain from the transmit IQ imbalance can be captured by using an optimal detector; however, the detection process requires an additional computational complexity on top of that required by an equalizer.

[2]It is worth to mention that the proposed algorithm is valid for any other transmit and receive IQ model. One just needs to plug in the desired model in our equations. However, for the presentation purpose, we employ a frequency-flat model and a frequency-selective model at the transmitter and receiver, respectively.

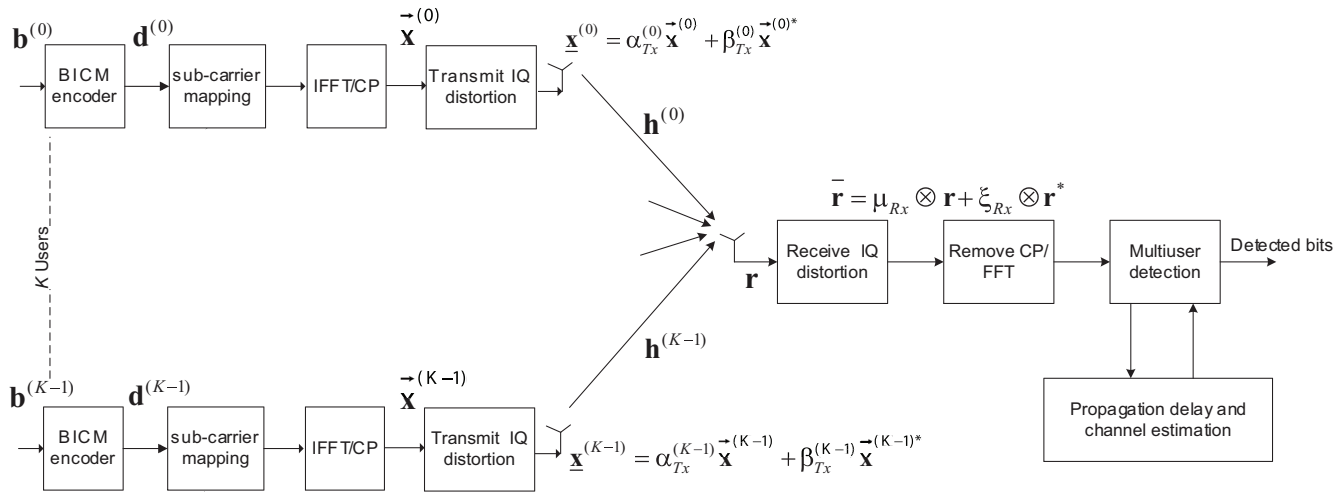

Fig. 1. OFDMA system with IQ imbalance.

incorporated in the CIR, which is the cascade of the transmit filter, the physical channel, and the receive filter, as assumed in many other studies (e.g., [6], [23]). Taking into account that $\tau^{(k)} \in \{0, 1, \cdots, \tau_{\max}\}$, where $\tau_{\max}$ is the maximum propagation delay, the samples taken prior to $-\nu$ and later than $M(N+\nu)+\tau_{\max}+L-\nu-2$ do not depend on the current frame[3]. Accordingly, the received frame

$$\mathbf{r} = [r(-\nu), \cdots, r\left(M(N+\nu)+\tau_{\max}+L-\nu-2\right)]$$

contains sufficient information for data detection and parameter estimation for each user. Mathematically, we can write

$$\mathbf{r} = \sum_{k=0}^{K-1} \overline{\mathbf{x}}^{(k)}\left(\tau^{(k)}\right) \otimes \mathbf{h}^{(k)} + \mathbf{n}, \tag{5}$$

where $\overline{\mathbf{x}}^{(k)}\left(\tau^{(k)}\right) = \left[\mathbf{0}_{1\times\tau^{(k)}}\, \underline{\mathbf{x}}^{(k)}\right]$ with $\mathbf{0}_{1\times\tau^{(k)}}$ as the all-zero vector of length $\tau^{(k)}$, $\otimes$ refers to convolution, and $\mathbf{n}$ is the noise vector. By applying the frequency-selective IQ parameters on the received frame, the distorted received sequence $\overline{\mathbf{r}}$ can be written as [7]

$$\overline{\mathbf{r}} = \boldsymbol{\mu}_{Rx} \otimes \mathbf{r} + \boldsymbol{\xi}_{Rx} \otimes \mathbf{r}^*, \tag{6}$$

where $\boldsymbol{\mu}_{Rx} = [\mu_{Rx}(0), \cdots, \mu_{Rx}(F-1)]$ and $\boldsymbol{\xi}_{Rx} = [\xi_{Rx}(0), \cdots, \xi_{Rx}(F-1)]$ are the distortion parameters associated with the frequency-selective IQ imbalance model, and

$$\mu_{Rx}(f) = \left(\left(\frac{1+\varepsilon_{Rx}}{2}\right) g_I(f) e^{-j\phi_{Rx}} + \left(\frac{1-\varepsilon_{Rx}}{2}\right) g_Q(f) e^{j\phi_{Rx}}\right), \tag{7a}$$

$$\xi_{Rx}(f) = \left(\left(\frac{1+\varepsilon_{Rx}}{2}\right) g_I(f) e^{j\phi_{Rx}} - \left(\frac{1-\varepsilon_{Rx}}{2}\right) g_Q(f) e^{-j\phi_{Rx}}\right). \tag{7b}$$

Here $f = 0, \cdots, F-1$ and F is the length of the impulse responses of the imperfect filters $g_I(f)$ and $g_Q(f)$ on the I and Q branches[4], and ε_{Rx} and ϕ_{Rx} represent the gain and phase imbalance at the receiver, respectively.

The goal of the receiver is to recover the transmitted information of K users. It is clear that this requires knowledge of the transmit IQ imbalance, the propagation delay, and CIR for each user, and the receive IQ imbalance. In order to solve the problem, we reformulate the previous equations. By using (3) and (6), and after simple mathematical manipulations, we can write

$$\overline{\mathbf{r}} = \sum_{k=0}^{K-1} \left(\left[\mathbf{0}_{1\times\tau^{(k)}}\, \vec{\mathbf{x}}^{(k)}\right] \otimes \hbar_0^{(k)} + \left[\mathbf{0}_{1\times\tau^{(k)}}\, \vec{\mathbf{x}}^{(k)*}\right] \otimes \hbar_1^{(k)}\right) + \mathbf{w}', \tag{8}$$

where $\mathbf{w}'$ is the noise contribution and

$$\hbar_0^{(k)} = \boldsymbol{\alpha}_{Tx}^{(k)} \boldsymbol{\mu}_{Rx} \otimes \mathbf{h}^{(k)} + \boldsymbol{\beta}_{Tx}^{(k)*} \boldsymbol{\xi}_{Rx} \otimes \mathbf{h}^{(k)*}, \tag{9a}$$

$$\hbar_1^{(k)} = \boldsymbol{\beta}_{Tx}^{(k)} \boldsymbol{\mu}_{Rx}^* \otimes \mathbf{h}^{(k)*} + \boldsymbol{\alpha}_{Tx}^{(k)} \boldsymbol{\xi}_{Rx}^* \otimes \mathbf{h}^{(k)}. \tag{9b}$$

One can show that (8) can be written in a matrix form as

$$\overline{\mathbf{r}} = \sum_{k=0}^{K-1} \left(\mathbf{S}_{\tau^{(k)}}^{(k)} \hbar_0^{T(k)} + \mathbf{S}_{\tau^{(k)}}^{(k)*} \hbar_1^{T(k)}\right) + \mathbf{w}', \tag{10}$$

where the subscript T denotes the vector transpose and

$$\mathbf{S}_{\tau^{(k)}}^{(k)} = \begin{bmatrix} \mathbf{0}_{\tau^{(k)}\times(L+F-1)} \\ \mathbf{S}^{(k)} \\ \mathbf{0}\left(\tau_{\max} - \tau^{(k)} + L + F - 2\right) \times (L+F-1) \end{bmatrix}. \tag{11}$$

Here $\mathbf{0}_{\beta_1\times\beta_2}$ denotes the all-zero matrix of size $\beta_1 \times \beta_2$ and $\mathbf{S}^{(k)}$ is an $(M(N+v)+L+F-2)\times(L+F-1)$ Toeplitz matrix constructed as

$$\mathbf{S}^{(k)} = \begin{bmatrix} x_0^{(k)} & 0 & 0 & 0 & 0 \\ x_1^{(k)} & x_0^{(k)} & 0 & 0 & 0 \\ x_2^{(k)} & x_1^{(k)} & x_0^{(k)} & 0 & 0 \\ \vdots & \vdots & \vdots & \vdots & \vdots \\ x_c^{(k)} & x_{c-1}^{(k)} & x_{c-2}^{(k)} & \cdots & x_{c-L-F-2}^{(k)} \\ 0 & x_c^{(k)} & x_{c-1}^{(k)} & \cdots & x_{c-L-F-1}^{(k)} \\ \vdots & \vdots & \vdots & \vdots & \vdots \\ 0 & 0 & 0 & 0 & x_c^{(k)} \end{bmatrix}, \tag{12}$$

[3]Note that in cellular communication systems, $\tau_{\max}$ depends on the cell radius and does not depend on the user index k [6].

[4]The frequency-selective IQ imbalance at the receiver primarily caused by imperfections in base-band and RF chains (including analog filters, amplifiers, mixers, and digital-to-analog converter) is typically modeled by filters [7]. Such filters for the I and Q branches of the receive antenna are denoted by $g_I(f)$ and $g_Q(f)$, $f = 0, 1, \cdots, F-1$. Note that this does not depend on the user index k.

$$\left[\hat{\mathbf{h}}_{eq}^{(0)},\cdots,\hat{\mathbf{h}}_{eq}^{(K-1)},\hat{\tau}^{(0)},\cdots,\hat{\tau}^{(K-1)}\right] = \arg\max_{\mathbf{h}_{eq}^{(0)},\cdots,\mathbf{h}_{eq}^{(K-1)},\tau^{(0)},\cdots,\tau^{(K-1)}} \log\left\{\Pr\left(\overline{\mathbf{r}}\left|\mathbf{h}_{eq}^{(0)},\cdots,\mathbf{h}_{eq}^{(K-1)},\tau^{(0)},\cdots,\tau^{(K-1)}\right.\right)\right. \tag{14}$$

$$\Pr\left(\overline{\mathbf{r}}\left|\mathbf{h}_{eq}^{(0)},\cdots,\mathbf{h}_{eq}^{(K-1)},\tau^{(0)},\cdots,\tau^{(K-1)}\right.\right) = \sum_{\mathbf{\Upsilon}_{\tau^{(0)}}^{(0)},\cdots,\mathbf{\Upsilon}_{\tau^{(K-1)}}^{(K-1)}} \Pr\left(\overline{\mathbf{r}}\left|\mathbf{\Upsilon}_{\tau^{(0)}}^{(0)},\cdots,\mathbf{\Upsilon}_{\tau^{(K-1)}}^{(K-1)},\mathbf{h}_{eq}^{(0)},\cdots,\mathbf{h}_{eq}^{(K-1)}\right.\right) \times \Pr\left(\mathbf{\Upsilon}_{\tau^{(0)}}^{(0)},\cdots,\mathbf{\Upsilon}_{\tau^{(K-1)}}^{(K-1)}\right) \tag{15}$$

$$\Pr\left(\overline{\mathbf{r}}\left|\mathbf{\Upsilon}_{\tau^{(0)}}^{(0)},\cdots,\mathbf{\Upsilon}_{\tau^{(K-1)}}^{(K-1)},\cdots,\mathbf{h}_{eq}^{(0)},\cdots,\mathbf{h}_{eq}^{(K-1)}\right.\right) \propto \left(-\frac{1}{\sigma_n^2}\left(\overline{\mathbf{r}}-\sum_{k=0}^{K-1}\mathbf{\Upsilon}_{\tau^{(k)}}^{(k)}\mathbf{h}_{eq}^{(k)}\right)^H\left(\overline{\mathbf{r}}-\sum_{k=0}^{K-1}\mathbf{\Upsilon}_{\tau^{(k)}}^{(k)}\mathbf{h}_{eq}^{(k)}\right)\right) \tag{16}$$

where $c = M(N+v)-1$ and $\left\{x_i^{(k)}\right\}_{i=0}^{c}$ are the elements of the transmitted frame of user k, $\vec{\mathbf{x}}^{(k)}$, given in (2). Furthermore, (10) can be simply expressed as

$$\overline{\mathbf{r}} = \sum_{k=0}^{K-1}\mathbf{\Upsilon}_{\tau^{(k)}}^{(k)}\mathbf{h}_{eq}^{(k)} + \mathbf{w}', \tag{13}$$

where $\mathbf{\Upsilon}_{\tau^{(k)}}^{(k)} = \left[\mathbf{S}_{\tau^{(k)}}^{(k)}\ \mathbf{S}_{\tau^{(k)}}^{(k)*}\right]$ and $\mathbf{h}_{eq}^{(k)} = \left[\hbar_0^{(k)}\ \hbar_1^{(k)}\right]^T$.

By using these transformations, we can estimate the overall CIR, $\mathbf{h}_{eq}^{(k)}$, as a single parameter, instead of estimating five parameters, $\left[\boldsymbol{\alpha}_{Tx}^{(k)}\,\boldsymbol{\beta}_{Tx}^{(k)},\boldsymbol{\mu}_{Rx}\,\boldsymbol{\xi}_{Rx}\,\mathbf{h}^{(k)}\right]$, for each user. We will show in Section IV that proper data detection can be performed if estimates of $\mathbf{h}_{eq}^{(k)}$ and $\tau^{(k)}$ are available.

III. Estimation Algorithm

The ML estimates of $\mathbf{h}_{eq}^{(k)}$ and $\tau^{(k)}$, $k = 0,1,\cdots,K-1$, are obtained by maximizing the log-likelihood function given in (14), where $\Pr(\diamondsuit|\heartsuit)$ is defined as the probability density function of $\diamondsuit$ given $\heartsuit$, and $\hat{\diamondsuit}$ denotes the estimated value of $\diamondsuit$. Evaluation of $\Pr\left(\overline{\mathbf{r}}\left|\mathbf{h}_{eq}^{(0)},\cdots,\mathbf{h}_{eq}^{(K-1)},\tau^{(0)},\cdots,\tau^{(K-1)}\right.\right)$ requires averaging over all transmitted data symbols as in (15). Using (13), one can write (16), where the superscript H denotes the Hermitian transpose and σ_n^2 is the additive white Gaussian noise (AWGN) variance. Here we follow the common assumption associated with most of the IQ estimation algorithms found in the literature that the noise, after being subject to the receive frequency-dependent IQ imbalance, is approximately treated as being zero-mean white Gaussian with variance σ_n^2 (e.g., [24]–[26]).

As one can observe from (14), (15), and (16), finding the ML estimate is intractable in practice, because it requires the averaging over all possible transmitted data sequences and the maximization over a large dimensional parameter set. For multi–dimensional parameter estimation, the SAGE algorithm [22] provides an iterative solution to find the ML estimate in the presence of nuisance parameters. In the following, we give a brief outline of the SAGE algorithm and apply it to the observation vector, $\overline{\mathbf{r}}$, to estimate the overall CIRs and the propagation delays of the K users.

A. Basic Principle

In many statistical problems, direct maximization of the ML likelihood function is often analytically challenging. The expectation-maximization (EM) algorithm can provide the ML solution with a comparatively simpler iterative procedure. The EM algorithm iteratively alternates between an E-step, calculating the log-likelihood function of the complete data[5], and an M-step, maximizing the expectation with respect to unknown parameters [27]. The parameter estimates are updated at each iteration, and the process continues until no significant changes in the updates are observed. The convergence of the EM algorithm is notoriously slow, especially for multidimensional parameter estimation, due to the simultaneous updating nature of the M-step. Thus, a large number of iterations may be required to achieve an acceptable performance.

The SAGE algorithm has been proposed in [22] to improve the convergence rate of the EM algorithm for multidimensional parameter estimation. Instead of estimating all parameters at once, the SAGE algorithm breaks up the parameters into several non-overlapped sets (subspaces) and employs the EM algorithm to sequentially update each set.

Mathematically, assume we want to estimate $\boldsymbol{\theta}$, which contains many parameters, from an observation $\overline{\mathbf{r}}$ in the presence of nuisance parameters. We break up $\boldsymbol{\theta}$ into K non-overlapping subsets $\left\{\theta^{(0)},\theta^{(1)},\cdots,\theta^{(K-1)}\right\}$, where $\theta^{(k)} \subseteq \boldsymbol{\theta}$, and $\theta^{(\overline{k})} \doteq \boldsymbol{\theta} \setminus \theta^{(k)}$ ($\theta^{(\overline{k})}$ is the compliment of $\theta^{(k)}$, such that $\theta^{(k)} \cup \theta^{(\overline{k})} = \boldsymbol{\theta}$). Starting from an initial parameter estimate $\left\{\theta^{(0)}(0),\theta^{(1)}(0),\cdots,\theta^{(K-1)}(0)\right\}$, SAGE iterates between an expectation (E) step and a maximization (M) step as follows.

1) Select a parameter subset $\theta^{(k)}$ to be updated while the estimate of $\theta^{(\overline{k})}$ is left unchanged;
2) The E-step computes (17), where E and λ denote the statistical average and the λth iteration, respectively, $\Psi^{(k)}$ is the missing data that corresponds to $\theta^{(k)}$, and $\mathbf{u}^{(k)}$ is the observed data corresponding to the subset $\theta^{(k)}$.
3) The M-step is now given by

$$\begin{cases} \widehat{\theta^{(k)}}(\lambda+1) = \arg\max_{\theta^{(k)}}\left\{Q\left(\theta^{(k)}\left|\widehat{\boldsymbol{\theta}}(\lambda)\right.\right)\right\} \\ \widehat{\theta^{\overline{k}}}(\lambda+1) = \widehat{\theta^{\overline{k}}}(\lambda) \end{cases}. \tag{21}$$

Repeat steps 1, 2, and 3 for all possible parameter subsets. Convergence of the SAGE algorithm is assured in the sense that the likelihood of the estimates is non-decreasing [22].

[5]The complete data includes the observed (incomplete) data and unobserved (missing) data.

$$Q\left(\theta^{(k)}\left|\widehat{\boldsymbol{\theta}}(\lambda)\right.\right) = \mathrm{E}_{\Psi^{(k)}}\left[\log \Pr\left(\mathbf{u}^{(k)}\left|\Psi^{(k)},\theta^{(k)}\right.\right)\left|\mathbf{u}^{(k)},\theta^{(\overline{k})}(\lambda)\right.\right] = \int_{\Psi^{(k)}} \log \Pr\left(\mathbf{u}^{(k)}\left|\Psi^{(k)},\theta^{(k)}\right.\right)\Pr\left(\Psi^{(k)}\left|\mathbf{u}^{(k)},\theta^{(\overline{k})}(\lambda)\right.\right) d\Psi^{(k)} \tag{17}$$

$$\mathrm{E}\left[x_m^{(k)}(n)\left|\mathbf{z}^{(k)},\hat{\mathbf{h}}_{eq}^{(k)}(\lambda),\hat{\tau}^{(k)}(\lambda)\right.\right] = \frac{1}{\sqrt{N}}\sum_{p=0}^{P-1}\mathrm{E}\left[d_m^{(k)}(p)|\mathbf{z}^{(k)},\hat{\mathbf{h}}_{eq}^{(k)}(\lambda),\hat{\tau}^{(k)}(\lambda)\right] e^{j2\pi n u^{(k)}(p)/N} \tag{18}$$

$$\mathrm{E}\left[d_m^{(k)}(p)|\,\mathbf{z}^{(k)},\hat{\mathbf{h}}_{eq}^{(k)}(\lambda),\hat{\tau}^{(k)}(\lambda)\right] = \sum_{\varpi\in\Omega}\varpi \times \Pr\left(d_m^{(k)}(p)=\varpi\left|\mathbf{z}^{(k)},\hat{\mathbf{h}}_{eq}^{(k)}(\lambda),\hat{\tau}^{(k)}(\lambda)\right.\right) \tag{19}$$

$$\Pr\left(\mathbf{z}^{(k)}|\boldsymbol{\Upsilon}_{\tau^{(k)}}^{(k)},\mathbf{h}_{eq}^{(k)}\right) = \frac{1}{(\pi\sigma_n^2)^{L_r}}\exp\left(-\left\|\mathbf{z}^{(k)}-\boldsymbol{\Upsilon}_{\tau^{(k)}}^{(k)}\mathbf{h}_{eq}^{(k)}\right\|^2/\sigma_n^2\right) \tag{20}$$

$$\Lambda\left(v_m^{(k)}(g)=b\right) = \sum_{d_m^{(k)}(p)\in\Psi(g,b)}\Pr\left(d_m^{(k)}(p)\mid \mathbf{R}_m^{(k)}(u^{(k)}(p)),\mathbf{H}^{(k)}(u^{(k)}(p))\right) = \sum_{d_m^{(k)}(p)\in\Psi(g,b)}\sum_{d_m^{(k)}(p')}\Pr\left(\mathbf{D}_m^{(k)}(p,p')\left|\mathbf{R}_m^{(k)}(u^{(k)}(p)),\mathbf{H}^{(k)}(u^{(k)}(p))\right.\right) \tag{29}$$

$$\Pr\left(\mathbf{D}_m^{(k)}(p,p')\left|\mathbf{R}_m^{(k)}(u^{(k)}(p)),\mathbf{H}^{(k)}(u^{(k)}(p))\right.\right) = \frac{\Pr\left(\mathbf{R}_m^{(k)}(u^{(k)}(p))\left|\mathbf{D}_m^{(k)}(p,p'),\mathbf{H}^{(k)}(u^{(k)}(p))\right.\right)\Pr\left(\mathbf{D}_m^{(k)}(p,p')\right)}{\Pr\left(\mathbf{R}_m^{(k)}(u^{(k)}(p))\left|\mathbf{H}^{(k)}(u^{(k)}(p))\right.\right)} \tag{30}$$

$$\Pr\left(\mathbf{R}_m^{(k)}(u^{(k)}(p))\left|\mathbf{H}^{(k)}(u^{(k)}(p))\right.\right) = \sum_{\mathbf{D}_m^{(k)}(p,p')}\Pr\left(\mathbf{R}_m^{(k)}(u^{(k)}(p))\left|\mathbf{D}_m^{(k)}(p,p'),\mathbf{H}^{(k)}(u^{(k)}(p))\right.\right) \times \Pr\left(\mathbf{D}_m^{(k)}(p,p')\right) \tag{31}$$

$$\Pr\left(\mathbf{R}_m^{(k)}(u^{(k)}(p))\left|\mathbf{D}_m^{(k)}(p,p'),\mathbf{H}^{(k)}(u^{(k)}(p))\right.\right) = \frac{1}{\pi^2\sigma_n^4}e^{-\left\|\mathbf{R}_m^{(k)}(u^{(k)}(p))-\mathbf{D}_m^{(k)}(p,p')\mathbf{H}^{(k)}(u^{(k)}(p))\right\|^2/\sigma_n^2} \tag{32}$$

B. Proposed Estimation Algorithm

Now coming back to our case study, we make the following associations $\theta^{(k)} \longleftrightarrow \left[\mathbf{h}_{eq}^{(k)},\tau^{(k)}\right]$, i.e., we estimate the overall CIR and propagation delay for one user at a time. Starting from an initial estimate, $\left[\hat{\mathbf{h}}_{eq}^{(0)}(0),\cdots,\hat{\mathbf{h}}_{eq}^{(K-1)}(0),\hat{\tau}^{(k)}(0),\cdots,\hat{\tau}^{(k)}(0)\right]$ and applying the SAGE algorithm to the problem under consideration yields the following iterative procedure at iteration $\lambda+1$:

1) Select user k for which the estimates of the overall CIR and the propagation delay must be updated.
2) We define $\mathbf{z}^{(k)}$ as the received signal corresponding to user k which is obtained by performing time-domain multiple access interference cancellation to remove the contributions from all users except user k from the total received signal. Mathematically, we can write

$$\mathbf{z}^{(k)} = \overline{\mathbf{r}} - \sum_{k'=0,k'\neq k}^{K-1}\widetilde{\boldsymbol{\Upsilon}}_{\hat{\tau}^{(k)}(\lambda)}^{(k')}\hat{\mathbf{h}}_{eq}^{(k')}(\lambda), \tag{22}$$

and $\widetilde{\boldsymbol{\Upsilon}}_{\hat{\tau}^{(k)}(\lambda)}^{(k')}$ is obtained by replacing each entry in $\boldsymbol{\Upsilon}_{\hat{\tau}^{(k)}(\lambda)}^{(k')}$ with the corresponding a posteriori expectation. Equation (1) tells us that the a posteriori expectation of the transmitted sample $x_m^{(k)}(n)$ can be expressed as in (18) and (19). In the next section, we will show how the detector can compute $\Pr\left(d_m^{(k)}(p)=\varpi\left|\mathbf{z}^{(k)},\hat{\mathbf{h}}_{eq}^{(k)}(\lambda),\hat{\tau}^{(k)}(\lambda)\right.\right)$. Based on (13) and (22), one can write (20) ,where L_r is the length of $\mathbf{z}^{(k)}$. From (17) and (20), and dropping irrelevant terms, it can be shown that

$$Q\left(\mathbf{h}_{eq}^{(k)},\tau^{(k)}\left|\hat{\mathbf{h}}_{eq}^{(k)}(\lambda),\hat{\tau}^{(k)}(\lambda)\right.\right) \propto 2\Re\left(\mathbf{z}^{(k)H}\widetilde{\boldsymbol{\Upsilon}_{\tau^{(k)}}^{(k)}}\mathbf{h}_{eq}^{(k)}\right) - \mathbf{h}_{eq}^{(k)H}\widetilde{\boldsymbol{\Upsilon}_{\tau^{(k)}}^{(k)H}\boldsymbol{\Upsilon}_{\tau^{(k)}}^{(k)}}\mathbf{h}_{eq}^{(k)}, \tag{23}$$

where $\Re(\diamondsuit)$ is the real part of a complex number $\diamondsuit$, $\widetilde{\boldsymbol{\Upsilon}_{\tau^{(k)}}^{(k)}} = \mathrm{E}_{\boldsymbol{\Upsilon}_{\tau^{(k)}}^{(k)}}\left[\boldsymbol{\Upsilon}_{\tau^{(k)}}^{(k)}\left|\mathbf{z}^{(k)},\hat{\mathbf{h}}_{eq}^{(k)}(\lambda),\hat{\tau}^{(k)}(\lambda)\right.\right]$, and $\widetilde{\boldsymbol{\Upsilon}_{\tau^{(k)}}^{(k)H}\boldsymbol{\Upsilon}_{\tau^{(k)}}^{(k)}} = \mathrm{E}_{\boldsymbol{\Upsilon}_{\tau^{(k)}}^{(k)}}\left[\boldsymbol{\Upsilon}_{\tau^{(k)}}^{(k)H}\boldsymbol{\Upsilon}_{\tau^{(k)}}^{(k)}\left|\mathbf{z}^{(k)},\hat{\mathbf{h}}_{eq}^{(k)}(\lambda),\hat{\tau}^{(k)}(\lambda)\right.\right]$. Assuming data symbols are uncorrelated, then one can show that $\widetilde{\boldsymbol{\Upsilon}_{\tau^{(k)}}^{(k)H}\boldsymbol{\Upsilon}_{\tau^{(k)}}^{(k)}}$ can be approximated by $\widetilde{\boldsymbol{\Upsilon}_{\tau^{(k)}}^{(k)H}}\widetilde{\boldsymbol{\Upsilon}_{\tau^{(k)}}^{(k)}}$.

3) M-step: now we update the estimates of $\mathbf{h}_{eq}^{(k)}$ and $\tau^{(k)}$ as

$$\left[\hat{\mathbf{h}}_{eq}^{(k)}(\lambda+1), \hat{\tau}^{(k)}(\lambda+1)\right] = \arg\max_{\mathbf{h}_{eq}^{(k)}, \tau^{(k)}} \left\{ Q\left(\mathbf{h}_{eq}^{(k)}, \tau^{(k)} \middle| \hat{\mathbf{h}}_{eq}^{(k)}(\lambda), \hat{\tau}^{(k)}(\lambda)\right)\right\}. \tag{24}$$

For each value of $\tau^{(k)}$, the estimate of $\mathbf{h}_{eq}^{(k)}$ can be found in closed form by maximizing (23) as

$$\hat{\mathbf{h}}_{eq}^{(k)}(\lambda+1, \tau^{(k)}) = \left(\widetilde{\mathbf{\Upsilon}_{\tau^{(k)}}^{(k)H} \mathbf{\Upsilon}_{\tau^{(k)}}^{(k)}}\right)^{-1} \widetilde{\mathbf{\Upsilon}_{\tau^{(k)}}^{(k)H}} \mathbf{z}^{(k)}. \tag{25}$$

Using (23), (24), and (25), the estimated delay $\tau^{(k)}$ can be obtained by using a one-dimensional linear search as

$$\hat{\tau}^{(k)}(\lambda+1) = \operatorname*{argmax}_{\tau^{(k)}} \left\{ -\mathbf{h}_{eq}^{(k)H}(\lambda+1, \tau^{(k)}) \widetilde{\mathbf{\Upsilon}_{\tau^{(k)}}^{(k)H} \mathbf{\Upsilon}_{\tau^{(k)}}^{(k)}} \mathbf{h}_{eq}^{(k)}(\lambda+1, \tau^{(k)}) + 2\Re\left(\mathbf{z}^{(k)H} \widetilde{\mathbf{\Upsilon}_{\tau^{(k)}}^{(k)}} \mathbf{h}_{eq}^{(k)}(\lambda+1, \tau^{(k)})\right)\right\}. \tag{26}$$

Finally, the estimated channel taps

$$\hat{\mathbf{h}}_{eq}^{(k)}(\lambda+1) = \hat{\mathbf{h}}_{eq}^{(k)}(\lambda+1, \hat{\tau}^{(k)}(\lambda+1)), \tag{27}$$

can be obtained by replacing $\tau^{(k)}$ by $\hat{\tau}^{(k)}(\lambda+1)$ in (25).

4) The previous steps are repeated for all users during the iteration process.

The following remarks are of interest:

- Every time we update $\mathbf{h}_{eq}^{(k)}$ and $\tau^{(k)}$, we need to re-compute the a posteriori probabilities $\Pr\left(d_m^{(k)}(p) \middle| \mathbf{z}^{(k)}, \hat{\mathbf{h}}_{eq}^{(k)}(\lambda), \hat{\tau}^{(k)}(\lambda)\right)$. This requires resetting the BICM detector and performing many detection iterations. We use the embedded estimation procedure [28] to avoid this overhead: when the parameters $\mathbf{h}_{eq}^{(k)}$ and $\tau^{(k)}$ are updated, the BICM detector is not reset, but keeps the extrinsic and a priori probabilities from the previous iteration of the BICM detector. In this case, the overhead related to the proposed SAGE estimation algorithm becomes reasonable.
- The initial values for the propagation delays and CIRs can be estimated from (26) and (27) by using the entries in (12) corresponding to the contribution of the pilot symbols only.

IV. Proposed Detector

As one can observe from (19), computing $\mathrm{E}\left[d_m^{(k)}(p) | \mathbf{z}^{(k)}, \hat{\mathbf{h}}_{eq}^{(k)}(\lambda), \hat{\tau}^{(k)}(\lambda)\right]$ is essential for the estimator. In this section, we show how the proposed detector computes this probability. Furthermore, we illustrate how the estimate of $\mathbf{h}_{eq}$ and $\tau^{(k)}$ can be used in the detection process. Unlike the existing literature of OFDMA in which the IQ effect is seen as a source of performance degradation and equalization to remove the IQ effect is required, our proposed detector exploits this unwanted effect to provide a diversity gain, without the necessity of an additional equalizer. For notation simplicity, we drop the superscript ˆ and the iteration index λ from the channel coefficients.

The conceptual block diagram of the proposed detector and channel estimator at the base station is shown in Figure 2. As the users have different locations, each user undergoes a different propagation delay. This leads to a loss of sub-carrier orthogonality, which translates into MAI and results in a degradation of the performance [6]. Therefore, we must remove the MAI in the time domain, as shown in (22). After MAI cancellation, we switch to the frequency domain to perform single user data detection. To perform data detection for user k, the base station splits its corresponding signal $\mathbf{z}^{(k)}$, given in (22), into M blocks, discards the first ν samples of each block, and takes an N-point FFT of the result. We can write the $\{u^{(k)}(p)\}$th bin of the FFT of the mth OFDMA block as

$$\begin{aligned} R_m^{(k)}(u^{(k)}(p)) &= d_m^{(k)}(p) H_0^{(k)}(u^{(k)}(p)) \\ &+ d_m^{(k)*}(p') H_1^{(k)*}(-u^{(k)}(p)) \\ &+ W_m^{(k)}(u^{(k)}(p)), \end{aligned} \tag{28}$$

where $H_0^{(k)}(\diamondsuit)$ and $H_1^{(k)}(\diamondsuit)$ are the $\diamondsuit$th output of the N-point FFT of $\hbar_0^{(k)}$ and $\hbar_1^{(k)}$ respectively, $d_m^{(k)}(p')$ is the data symbol on the sub-carrier $-u^{(k)}(p)$, and $W_m^{(k)}(\diamondsuit)$ is the noise contribution which includes a thermal noise component as well as the MAI at the first iteration or residual (uncanceled) MAI at every subsequent iteration. The received symbol $R_m^{(k)}(u^{(k)}(p))$ and its conjugate mirror $R_m^{*(k)}(-u^{(k)}(p))$ can be written in a matrix form as

$$\mathbf{R}_m^{(k)}(u^{(k)}(p)) = \mathbf{H}^{(k)}(u^{(k)}(p)) \mathbf{D}_m^{(k)}(p, p') + \mathbf{W}_m^{(k)}(u^{(k)}(p)), \tag{33}$$

where

$\mathbf{R}_m^{(k)}(u^{(k)}(p)) = \left[R_m^{(k)}(u^{(k)}(p)),\, R_m^{(k)}(-u^{(k)}(p))\right]^T$,

$\mathbf{D}_m^{(k)}(p, p') = \left[d_m^{(k)}(p),\, d_m^{*(k)}(p')\right]^T$,

$\mathbf{W}_m^{(k)}(u^{(k)}(p)) = \left[W_m^{(k)}(u^{(k)}(p)),\, W_m^{(k)}(-u^{(k)}(p))\right]^T$, and

$$\mathbf{H}^{(k)}(u^{(k)}(p)) = \begin{bmatrix} H_0^{(k)}(u^{(k)}(p)) & H_1^{*(k)}(-u^{(k)}(p)) \\ H_1^{(k)}(u^{(k)}(p)) & H_0^{*(k)}(-u^{(k)}(p)) \end{bmatrix}.$$

Following [29]–[32], the bit metric, $\Lambda\left(v_m^{(k)}(g) = b\right)$, can be computed as in (29), where the subset $\Psi(g, b) = \left\{\mu\left(\left[v_m^{(k)}(0), v_m^{(k)}(1), \cdots, v_m^{(k)}(G-1)\right] \mid v_m^{(k)}(g) = b\right)\right\}$, $\left[v_m^{(k)}(0), v_m^{(k)}(1), \cdots, v_m^{(k)}(G-1)\right]$ are the G bits corresponding to the symbol $d_m^{(k)}(p)$, μ is the labeling map, $g = 0, 1, \cdots, G-1$, and $b = 0, 1$. Based on the Bayes' theorem, we obtain (30), (31), and (32). Assuming that $d_m^{(k)}(p)$ and $d_m^{(k)}(p')$, $p \neq p'$, are statistically independent, $\Pr\left(\mathbf{D}_m^{(k)}(p, p')\right)$ can be expressed as

$$\Pr\left(\mathbf{D}_m^{(k)}(p, p')\right) = \Pr\left(d_m^{(k)}(p)\right) \Pr\left(d_m^{(k)}(p')\right). \tag{34}$$

After de-interleaving, the bit metrics are passed to the decoder to provide the a posteriori probabilities of the coded bits. These probabilities are interleaved and forwarded to the symbol a posteriori computation unit. Assuming that $v_m^{(k)}(0)$, $v_m^{(k)}(1), \cdots, v_m^{(k)}(G-1)$ are independent by using a good interleaver, the symbol a posteriori probability $\Pr\left(d_m^{(k)}(p)\right)$

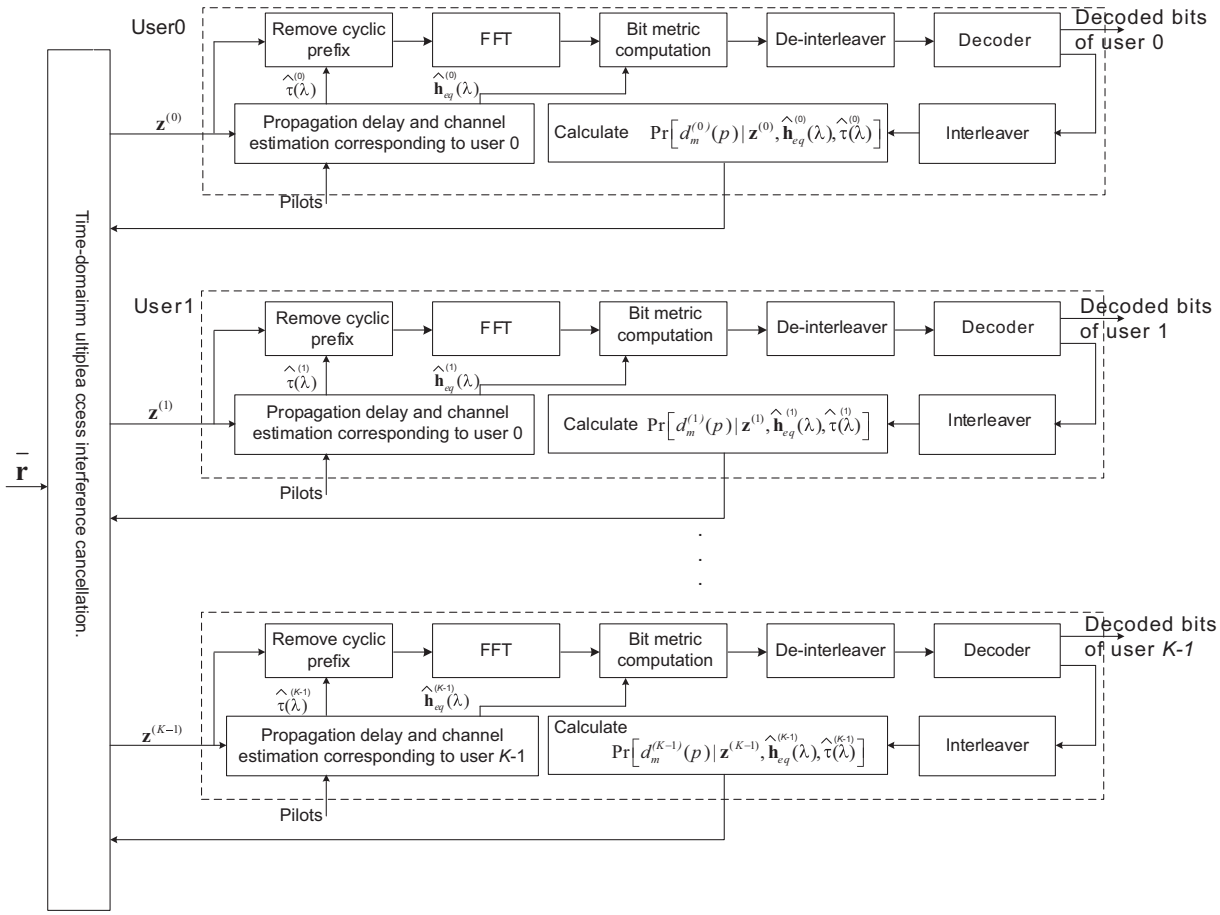

Fig. 2. Proposed detector and channel estimator at the base station.

can be computed as

$$\Pr\left(d_m^{(k)}(p)\right) = \prod_{g=0}^{G-1} \Pr\left(v_m^{(k)}(g)\right). \tag{35}$$

These a posteriori symbol probabilities are provided to the proposed estimator and MAP algorithms as a priori information, as indicated in (19) and in (30), respectively. At the last iteration, the final decoded outputs are the hard decisions based on the a posteriori probabilities.

V. Computational Complexity Analysis

In this section, we provide a computational complexity analysis of the proposed SAGE-based estimation algorithm and the proposed detector. The computational cost is evaluated in terms of the number of floating operations (flops) required for estimation and detection, with the multiplication and addition of two complex numbers requiring 6 and 2 flops, respectively [33][6]. In addition, we assume that the N-point FFT algorithm requires $5N\log_2(N)$ flops [34], multiplication of two complex matrices whose dimensions $\beta_1 \times \beta_2$ and $\beta_2 \times \beta_3$ requires $8\beta_1\beta_2\beta_3$ flops, addition/subtraction of two complex matrices, each has dimension of $\beta_1 \times \beta_2$, requires $2\beta_1\beta_2$ flops, and the inverse of a complex matrix with dimension $\beta_2 \times \beta_2$ needs β_2^3 flops [33]. Applying these into (22) - (27), one can compute the number of flops, C_{est}, per iteration per user of the proposed estimation algorithm of section (III) as

$$\begin{aligned} C_{est} &= 2\beta_1 + 8\left(K-1\right)\beta_1\beta_2 + 5\left(K-1\right)\chi\beta_1\beta_2\log_2 N \\ &+ \tau_{max}\left(\beta_2^3 + 16\beta_2^2 + 24\beta_1\beta_2 + 8\beta_1 + 8\beta_2\right), \end{aligned} \tag{36}$$

where χ is the modulation order, $\beta_1 = M(N+\nu) + L + F + \tau_{max} - 2$, and $\beta_2 = 2\left(L+F-1\right)$. For practical values of the system parameters, we can approximate β_1 as MN and β_2 as $2\left(L+F\right)$. Taking into account that $\beta_1 \gg \beta_2$, C_{est} can be approximated by

$$\begin{aligned} C_{est} &\approx 5\left(K-1\right)\chi\beta_1\beta_2\log_2 N \\ &\approx 10\left(K-1\right)\left(L+F\right)\chi MN\log_2 N. \end{aligned} \tag{37}$$

A more detailed view of the computational complexity analysis of the proposed estimation algorithm is given in Table I. Note that each $N+\nu$ elements of $\boldsymbol{\Upsilon}_{\tau^{(k)}}^{(k)}$, whose dimension β_1 by β_2, results from a single FFT process and requires $5\chi N\log_2 N$ flops as indicated in (18) and (19). Thus, in case of $N \gg \nu$, $\boldsymbol{\Upsilon}_{\tau^{(k)}}^{(k)}$ requires approximately $5\chi\beta_1\beta_2\log_2 N$ flops. In addition, the complexity of (27) is τ_{max} times the complexity of (25). We also notice that $\left(\boldsymbol{\Upsilon}_{\tau^{(k)}}^{(k)H}\boldsymbol{\Upsilon}_{\tau^{(k)}}^{(k)}\right)^{-1}$ is a common factor in (25) and (26), therefore this factor can be computed once; its complexity is included in (26).

Existing technology appears to be adequate for the practical implementation of the algorithm. For example, field programmable gate arrays (FPGAs) can readily achieve several

[6]Floating-point operations include any operations that involve fractional numbers.

TABLE I
COMPUTATIONAL COMPLEXITY OF THE PROPOSED ESTIMATION ALGORITHM PER ITERATION PER USER.

Computation	Complexity (flops per iteration per user)
$\widetilde{\boldsymbol{\Upsilon}}^{(k)}_{\tau^{(k)}}$	$5\chi\beta_1\beta_2\log_2 N$
$\widetilde{\left(\boldsymbol{\Upsilon}^{(k)H}_{\tau^{(k)}}\boldsymbol{\Upsilon}^{(k)}_{\tau^{(k)}}\right)}^{-1}$	$8\beta_1\beta_2+\beta_2^3$
Interference cancellation, (22)	$2\beta_1+8\left(K-1\right)\beta_1\beta_2+5\left(K-1\right)\chi\beta_1\beta_2\log_2 N$
Timing update, (26)	$\tau_{max}\left(8\beta_1\beta_2+\beta_2^3+8\beta_1+8\beta_1\beta_2+8\beta_2+8\beta_2^2\right)$
Channel update, (27)	$\tau_{max}\left(8\beta_1\beta_2+8\beta_2^2\right)$

Gigaflops per second [35], [36] provided the potential parallelism is effectively exploited, and highly optimized FPGA implementations of the FFT are available. Consider $M=10$, $N=64$, $\chi=4$, $K=4$, $L=4$, $F=2$, and FPGA with 5 Gigaflops per second, this provides C_{est} = 3686400 flops which leads to a computation time of 0.7 ms. Obviously, this processing time appears possible for practical implementation.

Following a similar approach, one can obtain the number of flops per iteration per user, C_{det}, required for the proposed detector as

$$C_{det}=46\chi\log_2\chi+\varpi',$$

where the first term results from the computational complexity of the proposed demapper, shown in (29), and the second term, ϖ', refers to the number of flops required for the decoder and interleaver; this depends on the code parameters such as constraint length, code rate, and generator polynomial. One can easily compute the numbers of flops for the traditional demapper (the demapper as if there is no IQ imbalance) given in [32] as $14\log_2\chi$ flops. Taking into account that ϖ' is common to the proposed detector and the traditional detector, the complexity of the proposed detector exceeds the traditional one by $(46\chi-14)\log_2\chi$ flops. In practice, this increase in complexity is not an issue with the existing technology. For example, if we consider $\chi=4$ with FPGA of 5 Gigaflops per second, an increase in computation time of 68 ns appears negligible in practice.

VI. SIMULATION RESULTS

To validate the proposed detection and estimation algorithms, we have carried out Monte Carlo simulations. We considered a BICM-OFDMA system, using a convolutional code with constraint length 5, rate $R=1/2$ and polynomial generators $(23)_8$ and $(35)_8$. The interleaved sub-carrier assignment was used. The number of sub-carriers was $N=256$, the cyclic prefix was $\nu=16$, the number of users was $K=4$, and the number of sub-carriers assigned for each user was $V=\frac{N}{K}=64$. For each user, a block length of $N_b=1416$ information bits was chosen, leading to $N_c=2832$ coded bits. The coded bits were mapped onto a 16-QAM constellation resulting in $N_d=708$ data symbols. Pilots symbols of length $N_p=60$ were appended for initial channel parameter estimation. This sequence of $N_d+N_p=768$ (16-QAM) symbols was broken up into $M=12$ blocks of $P=64$ (16-QAM) symbols per block. The maximum number of sample-spaced channel taps among all channels, L, was eight. Each link between user k and the base station was modeled with independent components, $\left\{h^{(k)}(l)\right\}$, each being a zero-mean complex Gaussian random variable with an exponential power delay profile:

$$\sigma^2_{AB}(l)=\Xi_{AB}\exp\left(-l/5\right),\ l=0,\ldots,L_{AB}-1 \qquad (38)$$

where L_{AB} was randomly chosen between 1 and L, and Ξ_{AB} was chosen such that the average energy per sub-carrier was set to E_{sc}. For the links between user 1, user 2, user 3, user 4 and the base station, E_{sc} was 1, 1.05, 0.95, and 1.1, respectively. The maximum propagation delay was $\tau_{max}=30$. Frequency-flat and frequency-selective IQ imbalance models are used at the transmitters and receiver, respectively. In the latter model, the time-domain impulse responses of the imperfect filters in the I and Q branches are chosen as three-taps ($F=3$) 4th-order Chebyshev filter of type one. The IQ parameters are $\varepsilon^{(1)}_{Tx}=0.2$, $\varepsilon^{(2)}_{Tx}=0.4$, $\varepsilon^{(3)}_{Tx}=0.3$, $\varepsilon^{(2)}_{Tx}=0.15$, $\phi^{(1)}_{Tx}=4^o$, $\phi^{(2)}_{Tx}=6^o$, $\phi^{(3)}_{Tx}=1^o$, $\phi^{(4)}_{Tx}=5^o$, $\varepsilon_{Rx}=0.35$, and $\phi_{Rx}=2.5^o$.

To show the validity of the proposed detection algorithm, we first consider perfect channel knowledge at the receiver in the case of synchronous users[7], i.e., the users' signals are aligned in time. Figure 3 illustrates the bit-error-rate (BER) performance for the proposed detector as a function of E_b/N_0, where E_b and N_0 are the energy per bit and noise power spectral density, respectively. For the sake of comparison, we also show the BER in the case of perfect estimation and compensation for the IQ imbalance[8], and that with no compensation for the IQ imbalance. These results are obtained at iteration 7. As one can observe, if not compensated for, the IQ imbalance will result in an unacceptable BER performance. Our proposed detector that beneficially exploits the IQ imbalance, results in a diversity gain of about 3 dB at high E_b/N_0 values compared to the case of perfect estimation and compensation of IQ parameters. Note that the source of the diversity gain is the transmit IQ, not the receive IQ. This is because the transmit IQ imbalance leads to transmit the useful information through two components as in shown in (3) while the receive IQ affects the useful component and noise component in the same way.

Next, we consider joint channel and IQ imbalance estimation in the case of synchronous users. Figure 4 shows the mean square error (MSE) of the overall CIRs as a function of E_b/N_0. Furthermore, the MSE of an estimator which has perfect knowledge of all data symbols is also included. This serves as a lower bound on the MSE performance. As can be observed, an improvement of the MSE is iteratively achieved. The SAGE estimator is able to achieve the lower bound at high E_b/N_0 values after three iterations.

Figure 5 shows the BER performance of the proposed detector in conjunction with the SAGE-based estimation algo-

[7]Note that the base station can send back timing information to the users so that they can adjust their start times thereby ensuring that all incoming signals arrive at the base station at the same time.

[8]The BER of the case of perfect estimation and compensation for IQ imbalance is the BER of the case as if there is no IQ imbalance, i.e., $\boldsymbol{\alpha}^{(k)}_{Tx}=1$, $\boldsymbol{\beta}^{(k)}_{Tx}=0$, $\boldsymbol{\mu}_{Rx}=1$, and $\boldsymbol{\xi}_{Rx}=0$, $\forall k\in\{0,\cdots,K-1\}$.

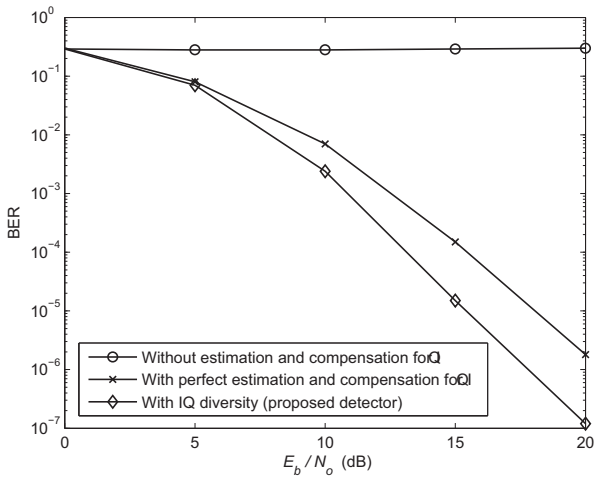

Fig. 3. BER performance comparison.

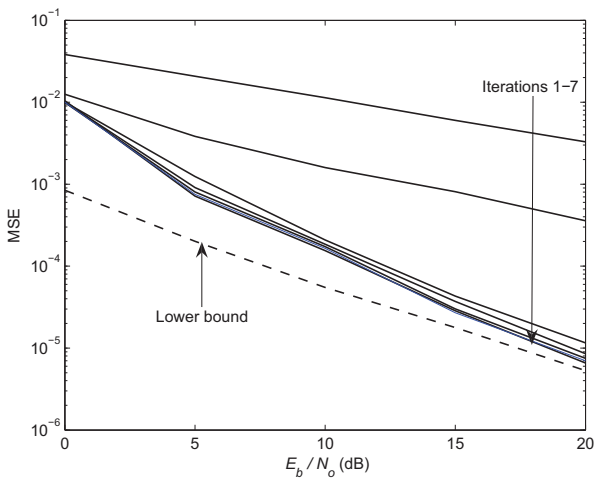

Fig. 4. MSE performance enhancement with the proposed SAGE algorithm.

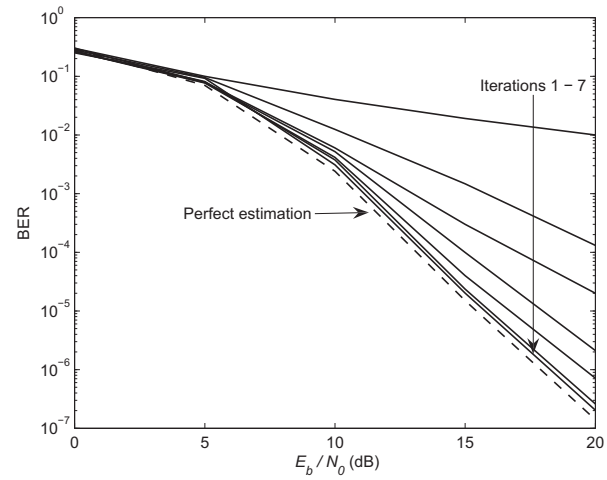

Fig. 5. BER performance of the proposed data detection algorithm in conjunction with the proposed estimation algorithm.

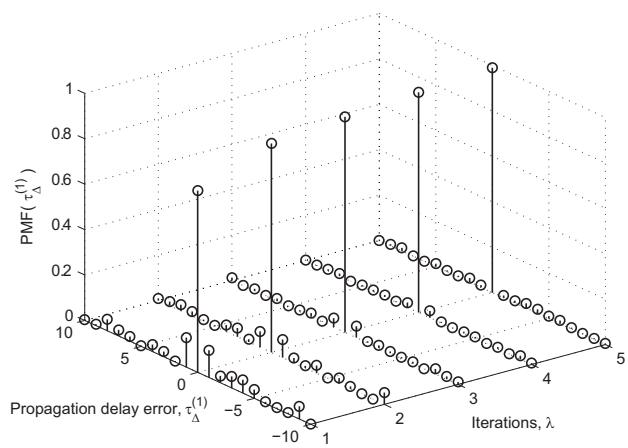

Fig. 6. PMF of the propagation delay error of the first user at $E_b/N_0 = 20$ dB.

rithm in the case of synchronous users. As can be observed, when performing data-aided channel estimation (i.e., the first iteration), the BER degradation is unacceptable as compared to the case of perfect estimation. The code-aided estimator is able to reduce this degradation to around 0.4 dB after 7 iterations. This can be explained as follows. In the first iteration, since the estimation process is based on a few pilots, the reliability of the soft information provided by the detector is low. However, when the number of iterations increases, the reliability of the estimation and data detection improves, as more information is employed compared to the first iteration.

Next, we consider joint propagation delay and overall channel estimation. Figure 6 depicts the probability mass function (PMF) of $\tau_\Delta^{(1)} = \hat{\tau}^{(1)} - \tau^{(1)}$ for the propagation delay of the first user at $E_b/N_0 = 20$ dB. Here we consider the first user ($k = 1$) as an asynchronous (new) user and the other three users are synchronous users. The propagation delays $\tau^{(k)}$ are fixed to 22, 18, 18, 18 for $k = 1, 2, 3, 4$, respectively, and the reference propagation delay is 18. As one can observe from the figure, the proposed estimation algorithm achieves a good performance; the PMF is almost one for $\tau_\Delta^{(1)} = 0$ at the fifth iteration.

Figure 7 shows the corresponding BER performance. Note that for the asynchronous user, we estimate the propagation delay and the overall CIR, and for the other three synchronous users, we only estimate the overall CIRs. As can be observed, an impressive performance gain results from exploiting the available soft information from the iterative decoder in the proposed estimator; only 0.8 dB BER performance loss occurs with respect to the BER performance of the case where the IQ imbalance is exploited as a beneficial resource and the receiver has perfect knowledge of the CIRs, IQ imbalance, and propagation delays.

Figure 8 shows the BER performance of the proposed detector in conjunction with the SAGE-based estimation algorithm as a function of the number of asynchronous users at $E_b/N_0 = 20$ dB. In this figure, the total number of users, $K = 4$, is the sum of the number of synchronous and asynchronous users, and their propagation delays $\{\tau^{(k)}\}$ are fixed to 22, 25, 28, 18 for $k = 1, 2, 3, 4$, respectively, and the reference propagation delay is 18. The results indicate that the BER performance slightly increases with the number of asynchronous users. This is because increasing the number of asynchronous users increases the MAI, which degrades the BER performance. In addition, we observe a significant

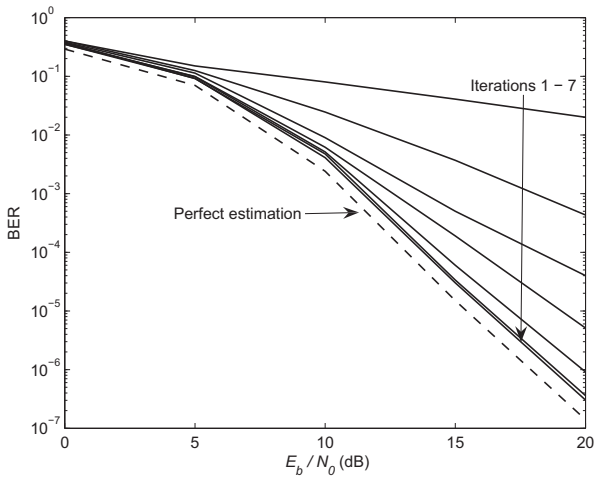

Fig. 7. BER performance of the proposed data detection algorithm in conjunction with the proposed estimation algorithm, one asynchronous user and three synchronous users.

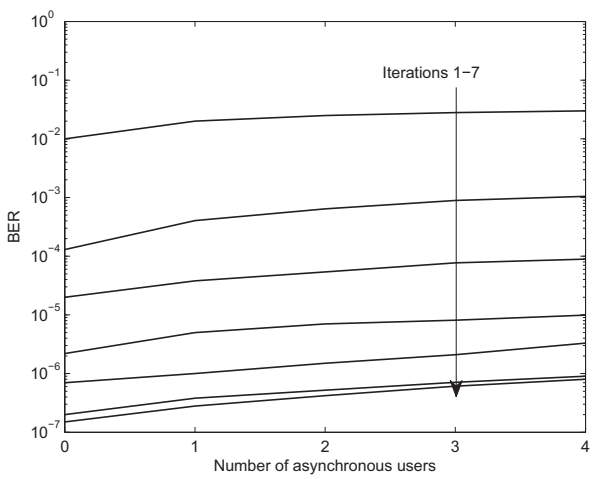

Fig. 8. BER performance of the proposed data detection algorithm in conjunction with the proposed estimation algorithm as a function of number of asynchronous users at $E_b/N_0 = 20$ dB.

performance improvement resulting from iterating between the proposed detector and estimator.

VII. Conclusion

We have proposed a SAGE-based algorithm for the problem of estimating the channel impulse response and both transmitters and receiver IQ imbalance for uplink asynchronous transmission of BICM-OFDMA systems. Furthermore, we have developed a novel demapper by exploiting the IQ imbalance as a beneficial resource to achieve a diversity gain, without the necessity of an additional equalizer. Results indicate that the BER performance of the proposed detector in conjunction with the proposed estimation algorithm is close to the BER of the perfect known parameters case with a diversity gain resulting from the IQ imbalance. Our proposed approach has several advantages:

- The proposed estimation algorithm exploits the iterative nature of the BICM decoder; the soft information resulting from the detector can be iteratively exploited to improve the estimation process. In addition, it can be employed with any detector as long as the detector is able to compute the a posteriori probabilities of the data symbols.
- The proposed estimation algorithm can be used instead of different independently operating algorithms to estimate the transmit and receive IQ imbalance for each user, to estimate the channels and propagation delays, and to perform equalization for the transmit and receive IQ imbalance, with acceptable computational cost.
- The proposed estimation algorithm is suitable for asynchronous transmission.
- The proposed detector achieves a diversity gain from the IQ imbalance, while maintaining approximately the same computational cost as the traditional detector that does not take into account the presence of the IQ imbalance. In addition, it requires neither channel equalization nor transmit and receive IQ imbalance equalization; this significantly saves processing time.

Although the proposed approach has proved itself as an efficient technique for handling the IQ imbalance, it has its own challenge:

- The estimation algorithm requires a quasi-static channel over the transmitted frame duration. Further research is required to modify the algorithm in order to fit time-varying channels.

Acknowledgment

The authors are grateful to the anonymous reviewers and the Editor, Prof. S. Wei, for their constructive comments.

References

[1] J. Andrews, A. Ghosh, and R. Muhamed, *Fundamentals of WiMAX: Understanding Broadband Wireless Network*. Prentice Hall, 2007.
[2] A. Ghosh, J. Zhang, J. Andrews, and R. Muhamed, *Fundamentals of LTE*. Prentice Hall, 2010.
[3] W. Huang, C. Pan, C. Li, and H. Li, "Subspace-based semi-blind channel estimation in uplink OFDMA systems," *IEEE Trans. Broadcast.*, vol. 56, no. 1, pp. 58–65, Mar. 2010.
[4] F. Suili and Y. Wu, "Pilot-assisted channel estimation method for OFDMA systems over time-varying channels," *IEEE Commun. Lett.*, vol. 13, no. 11, pp. 826–828, Nov. 2009.
[5] Y. Ma and R. Tafazolli, "Channel estimation for OFDMA uplink: a hybrid of linear and BEM interpolation approach," *IEEE Trans. Signal Process.*, vol. 55, no. 4, pp. 1568–1573, Apr. 2007.
[6] M. Morelli, "Timing and frequency synchronization for the uplink of an OFDMA system," *IEEE Trans. Commun.*, vol. 52, no. 2, pp. 296–296, Feb. 2004.
[7] F. Horlin and A. Bourdoux, *Digital Compensation for Analog Front-Ends*. Wiley, 2008.
[8] M. Windisch, "Estimation and compensation of IQ imbalance in broadband communication receivers," Ph.D. dissertation, Technische Universitat Dresden, Germany, 2007.
[9] A. Tarighat, R. Bagheri, and A. Sayed, "Compensation schemes and performance analysis of IQ imbalances in OFDM receivers," *IEEE Trans. Signal Process.*, vol. 53, no. 8, pp. 3257–3268, Aug. 2005.
[10] J. Tubbax, B. Come, L. Van der Perre, S. Donnay, M. Engels, H. De Man, and M. Moonen, "Compensation of IQ imbalance and phase noise in OFDM systems," *IEEE Trans. Wireless Commun.*, vol. 4, no. 3, pp. 872–877, May 2005.
[11] D. Tandur and M. Moonen, "Joint adaptive compensation of transmitter and receiver IQ imbalance under carrier frequency offset in OFDM-based systems," *IEEE Trans. Signal Process.*, vol. 55, no. 11, pp. 5246–5252, Nov. 2007.
[12] A. Tarighat and A. Sayed, "Joint compensation of transmitter and receiver impairments in OFDM systems," *IEEE Trans. Wireless Commun.*, vol. 6, no. 1, pp. 240–247, Jan. 2007.
[13] G. Gill, I. Sohn, J. Park, and Y. Lee, "Joint ML estimation of carrier frequency, channel, IQ mismatch, and DC offset in communication receivers," *IEEE Trans. Veh. Technol.*, vol. 54, no. 1, pp. 338–349, Jan. 2005.

[14] E. Estraviz, S. De Rore, F. Horlin, and L. Van der Perre, "Optimal training sequences for joint channel and frequency-dependent IQ imbalance estimation in OFDM-based receivers," in *Proc. 2006 IEEE International Conference on Communications*, pp. 4595–4600.

[15] W. Cho, T. Chang, Y. Chung, S. Phoong, and Y. Lin, "Frame synchronization and joint estimation of IQ imbalance and channel response for OFDM systems," in *Proc. 2008 IEEE International Conference on Acoustics, Speech, and Signal Processing*, pp. 3029–3032.

[16] E. Estraviz and L. Van der Perre, "EM based frequency-dependent transmit/receive IQ imbalance estimation and compensation in OFDM-based transceivers," in *Proc. 2007 IEEE Global Communications Conference*, pp. 4274–4279.

[17] F. Horlin, A. Bourdoux, and L. Van der Perre, "Low-complexity EM-based joint acquisition of the carrier frequency offset and IQ imbalance," *IEEE Trans. Wireless Commun.*, vol. 7, no. 6, pp. 2212–2220, June 2008.

[18] M. Inamori, A. Bostamam, Y. Sanada, and H. Minami, "IQ imbalance compensation scheme in the presence of frequency offset and dynamic DC offset for a direct conversion receiver," *IEEE Trans. Wireless Commun.*, vol. 7, no. 6, pp. 2214–2220, May 2009.

[19] I. Shon, E. Jeong, and Y. Lee, "Data-aided approach to IQ mismatch and DC offset compensation in communication receivers," *IEEE Commun. Lett.*, vol. 6, no. 12, pp. 547–549, Dec. 2002.

[20] Y. Yoshida, K. Hayashi, H. Sakai, and W. Bocquet, "Analysis and compensation of transmitter IQ imbalances in OFDMA and SC-FDMA systems," *IEEE Trans. Signal Process.*, vol. 57, no. 8, pp. 3119–3129, Mar. 2009.

[21] H. Mahmoud, H. Arslan, M. Kemal, and F. Retnasothie, "IQ imbalance correction for OFDMA uplink systems," in *Proc. 2009 IEEE International Conference on Communications*, pp. 1–5.

[22] J. A. Fessler and A. O. Hero, "Space alternating generalized expectation maximization algorithm," *IEEE Trans. Signal Process.*, vol. 42, no. 10, pp. 2664–2677, Oct. 1994.

[23] H. Meyr, S. Fechtel, and M. Moeneclaey, *Digital Communication Receivers: Synchronization, Channel Estimation, and Signal Processing*. Wiley, 1997.

[24] B. Narasimhan, D. Wang, S. Narayanan, H. Minn, and N. Al-Dhahir, "Digital compensation of frequency-dependent joint Tx/Rx I/Q imbalance in OFDM systems under high mobility," *IEEE J. Sel. Topics Signal Process.*, vol. 3, no. 3, pp. 405–417, June 2009.

[25] L. He, S. Ma, Y. Wu, Y. Zhou, T. Ng, and H. Poor, "Pilot-aided IQ imbalance compensation for OFDM systems operating over doubly selective channels," *IEEE Trans. Signal Process.*, vol. 59, no. 5, pp. 2223–2233, May 2011.

[26] V. Gottumukkala and H. Minn, "Capacity analysis and pilot-data power allocation for MIMO-OFDM with transmitter and receiver IQ imbalances and residual carrier frequency offset," *IEEE Trans. Veh. Technol.*, vol. PP, no. 99, pp. 1–12, Dec. 2011.

[27] T. Moon, "The expectation maximization algorithm," *IEEE Signal Process. Mag.*, vol. 13, no. 6, pp. 47–60, Nov. 1996.

[28] V. Lottici and M. Luise, "Embedding carrier phase recovery into iterative decoding of turbo-coded linear modulations," *IEEE Trans. Commun.*, vol. 52, no. 4, pp. 661–669, Apr. 2004.

[29] A. Chindapol and J. Ritcey, "Bit interleaved coded modulation with iterative decoding and 8PSK signaling," *IEEE Trans. Commun.*, vol. 50, no. 8, pp. 1250–1257, Aug. 2002.

[30] G. Caire, G. Taricco, and E. Biglieri, "Bit interleaved coded modulation," *IEEE Trans. Inf. Theory*, vol. 44, no. 3, pp. 927–946, May 1998.

[31] A. Chindapol and J. Ritcey, "Design, analysis and performance evaluation for BICM-ID with square QAM constellations in Rayleigh fading channels," *IEEE J. Sel. Areas Commun.*, vol. 19, no. 5, pp. 944–757, May 2001.

[32] X. Li and J. Ritcey, "Trellis-coded modulation with bit interleaving and iterative decoding," *IEEE J. Sel. Areas Commun.*, vol. 17, no. 4, pp. 715–724, Apr. 1999.

[33] S. Watkins, *Fundamentals of Matrix Computations*. Wiley, 2002.

[34] S. Johnson, and M. Frigo, "A modified split-radix FFT with fewer arithmetic operations," *IEEE Trans. Signal Process.*, vol. 55, no. 1, pp. 111–119, Jan. 2007.

[35] "Taking advantage of advances in FPGA floating-point IP cores." Available: http://www.altera.com/literature/wp/wp-01116-floating-point.pdf.

[36] A. Roldao and G. Constantinides, "A high throughput FPGA-based floating point conjugate gradient implementation for dense matrices," *ACM Trans. Reconfigurable Technol. Syst.*, vol. 3, no. 1, pp. 1–19, Jan. 2010.

Mohamed Marey received the M.Sc. and Ph.D. degrees in Electrical Engineering from Menoufyia University, Egypt, and Ghent University, Belgium, in 1999 and 2008, respectively. After that, he joined the Faculty of Engineering and Applied Science, Memorial University, Canada, as a research associate. Currently, he is an Assistant Professor at the Department of Electronics and Electrical Communications Engineering, Menoufyia University.

Dr. Marey received the young scientist award from International Union of Radio Science (URSI) in 1999. He is the author of the book Multi-carrier Receivers in the Presence of Interference: Overlay Systems (VDM Publishing House Ltd., 2009), and approximately 50 scientific papers published in international journals and conferences. His main research interests are in wireless communications and digital signal processing, with a particular focus on cooperative communications, cognitive radio systems, multiple-input multiple-output antenna systems, multi-carrier systems, synchronization and channel estimation, and error correcting codes.

Heidi Steendam (M'01-SM'06) received the M.Sc. degree in Electrical Engineering and the Ph.D. degree in Applied Sciences from Ghent University, Gent, Belgium in 1995 and 2000, respectively. Since September 1995, she has been with the Digital Communications (DIGCOM) Research Group, Department of Telecommunications and Information Processing (TELIN), Faculty of Engineering, Ghent University, Belgium, first in the framework of various research projects, and since October 2002 as a full time Professor in the area of Digital Communications.

Her main research interests are in statistical communication theory, carrier and symbol synchronization, bandwidth-efficient modulation and coding, spread-spectrum (multi-carrier spread-spectrum), satellite and mobile communication, cognitive radio and cooperative networks. She is the author of more than 125 scientific papers in international journals and conference proceedings.

Since 2002, she is an executive Committee Member of the IEEE Communications and Vehicular Technology Society Joint Chapter, Benelux Section, and since 2012 the vice chair. She has been active in various international conferences as Technical Program Committee chair/member and Session chair. In 2004 and 2011, she was the conference chair of the IEEE Symposium on Communications and Vehicular Technology in the Benelux. She is associate editor of IEEE TRANSACTIONS ON COMMUNICATIONS, *EURASIP Journal on Wireless Communications and Networking* and *Hindawi Journal of Computer Networks and Communications*.